2011

# Development, validation and verification of the Momentum Source Model for discrete rotor blades

Kanchan Guntupalli
*Iowa State University*

# CHAPTER 3. UNSTEADY ROTOR MODEL FOR DISCRETE BLADES

In the previous chapter, the modeling of the governing equations using a finite volume median-dual based methodology was discussed. In this chapter, the rotor modeling technique that is used in conjunction with the flow solver to simulate rotorcraft flows is described. The development of the rotor sources ($S'_x, S'_y, S'_z$) and their coupling with the discretized momentum conservation equations are explained.

## 3.1 Momentum Source Method

The present work uses the momentum source method to model the effect of a rotor [36]. According to the momentum source approach, which was first applied to vertical axis wind turbines, the function of a rotating rotor is to impart momentum to the flow. The rotor is, thus, replaced by distributed sources of momentum in the flow. The direction and magnitude of the imparted momentum depend on the rotor geometry and local flow characteristics. The advantages of this method are that it requires no apriori assumption about the wake structure and the need for a body-fitted rotor grid is also eliminated. Use of momentum sources to represent the rotor admittedly compromises the reality of the simulation very close to the surface by not resolving the (chord wise and span wise) boundary layer flow on the rotor. However, the versatility of the method that makes it compatible with a variety of flow solvers and its ability to solve rotorcraft flows economically has made this approach a very attractive technique for rotor modeling.

The original version of the rotor model using momentum source approach was steady in nature, wherein the spinning rotor was represented by time-averaged momentum sources. In the current work, a time-accurate, unsteady momentum source based rotor model, that has certain advantages over its earlier version, has been developed and implemented. Before we go into the details of the unsteady rotor model itself, it would be worthwhile to take a look at the steady rotor model and its scope.

## 3.2 Steady Rotor Model

In the steady rotor model, the rotor is treated as a solid disk with blades present throughout the rotor disk plane. The fact that a rotor is actually made up of discrete blades, which change position with time, is not taken into account. The rotor disk is discretized into concentric circles centered at the rotor center. The control volumes of the computational domain with which the entire rotor disk intersects are determined and this process is completed before the time iterations of the unsteady flow solver start and is not repeated again. At any given instant in time, the rotor forces are determined using the currently available velocity field. The question of where and how to add this rotor source term in the computational domain now arises. It must be noted here that a practical rotor is not a disk, but is made up of discrete blades. However, the steady rotor model does not consider the presence of discrete blades. It does not determine the instantaneous location of each rotor blade as the rotor rotates, instead approximates the blades to be present throughout the disk plane. This means that at every instant in time, the steady rotor model adds a unique source term to each control volume intersected by the entire disk plane. This results in time-averaging of the rotor's influence. For an $N_b$-bladed rotor, the time averaged rotor source term $\vec{S} = (S'_x, S'_y, S'_z)$ to be added to the discretized momentum equations is:

$$\vec{S} = \frac{N_b \Delta\theta}{2\pi}(-\vec{F}) \tag{3.1}$$

where, $\Delta\theta$ is the distance that a blade would travel while traversing through a control volume and $-\vec{F}$ is the instantaneous force acting on that control volume, which depends on the velocity field. The source term is averaged over $2\pi$ to account for the fact that the rotor has been modeled as a disk and this source term is now added to all the control volumes intersected by the rotor disk plane. Therefore, at every instant in time, the influence of the rotor is felt throughout the disk plane and this results in an averaged flow field. While such time-averaged momentum source modeling is adequate to predict overall blade loading, it is not capable of capturing the discrete unsteady features of a rotorcraft flow like blade passage effects. This leads to the need for a rotor model that accounts for discrete blade aerodynamics of a rotorcraft flow. Such a model has been developed in this work and the details are given in the following sections.

## 3.3 Unsteady Rotor Model for Discrete Blades

The effect of a rotating rotor is to impart momentum to the flow. The direction and magnitude of the imparted momentum depend on the characteristics of the rotating blades and the aerodynamic forces exerted by them. The process of evaluating such a momentum-based influence of the rotor can be broken down into two sub-processes. The first sub-process is to determine the region of the computational domain where such an influence has to be added. In the current research, this step is termed as finding the rotor "intersections" with the computational domain. The second task is to determine the magnitude of the rotor source itself that acts in these specific rotor intersected regions.

### 3.3.1 Coordinate Systems

The implementation of the above methodology requires the description of the rotor geometry, which is done by using four different coordinate systems. An explanation of these coordinate systems and mutual transformations between them are now presented.

#### 3.3.1.1 Computational Domain Coordinates

The governing equations are solved in an unstructured framework, where the three coordinate directions are denoted by $(x, y, z)$, with unit vectors $\hat{i}$, $\hat{j}$ and $\hat{k}$. In this system, the center of the rotor is designated by $(x_c, y_c, z_c)$ and the axis of rotation is perpendicular to the disk, along $\vec{\Omega}$ where

$$\vec{\Omega} = \Omega_1 \hat{i} + \Omega_2 \hat{j} + \Omega_3 \hat{k} \tag{3.2}$$

and $|\vec{\Omega}| = \Omega$ is the rotational speed in radians per second.

#### 3.3.1.2 Rotor Based Cartesian System

The computational coordinate system is aligned such that one axis is along the freestream velocity and the other two axes are mutually perpendicular to it. But the rotor is usually at an arbitrary orientation with respect to the freestream. This results in the need for a rotor based coordinate system that can be related to the computational coordinate system. The rotor based Cartesian coordinate system $(\xi, \eta, \zeta)$ has its origin at the rotor center and the axis $\xi$ points in the direction perpendicular to the rotor disk plane, as shown in Fig. 3.1. To form a mutually perpendicular right handed coordinate system, axes $\eta$ and $\zeta$ have to lie in the plane of the rotor. The transformation from this rotor based Cartesian coordinate system to the computational coordinate system can be achieved by first translating the origin and then using the method of Euler angle rotations. This is given below.

$$\begin{bmatrix} \xi \\ \eta \\ \zeta \end{bmatrix} = \begin{bmatrix} \cos B & \sin A \sin B & -\cos A \sin B \\ 0 & \cos A & \sin A \\ \sin B & -\sin A \cos B & \cos A \cos B \end{bmatrix} \times \begin{bmatrix} x - x_c \\ y - y_c \\ z - z_c \end{bmatrix} = \mathbf{M_1} \times \begin{bmatrix} x - x_c \\ y - y_c \\ z - z_c \end{bmatrix} \tag{3.3}$$

where, angle '$B$' denotes the tilt of the rotor with respect to the computational coordinate system and angle '$A$' denotes its sideslip. A rigorous derivation of the above transformation is given in Ref. [40].

#### 3.3.1.3 Rotor Based Cylindrical Polar Coordinate System

For the purpose of convenience in defining the rotor, we further define a rotor based cylindrical polar coordinate system $(r, \theta, z)$ as shown in Fig. 3.2. In this system, the $z$ axis is aligned along $\xi$, $r$ points radially outwards and $\theta$ is such that:

$$\theta = \frac{\pi}{2} - \psi \tag{3.4}$$

where, $\psi$ is the azimuthal angle of the rotor taken anticlockwise from the positive $x$ axis. The unit vectors in this system are related to those in the $(\xi, \eta, \zeta)$ system by the following matrix

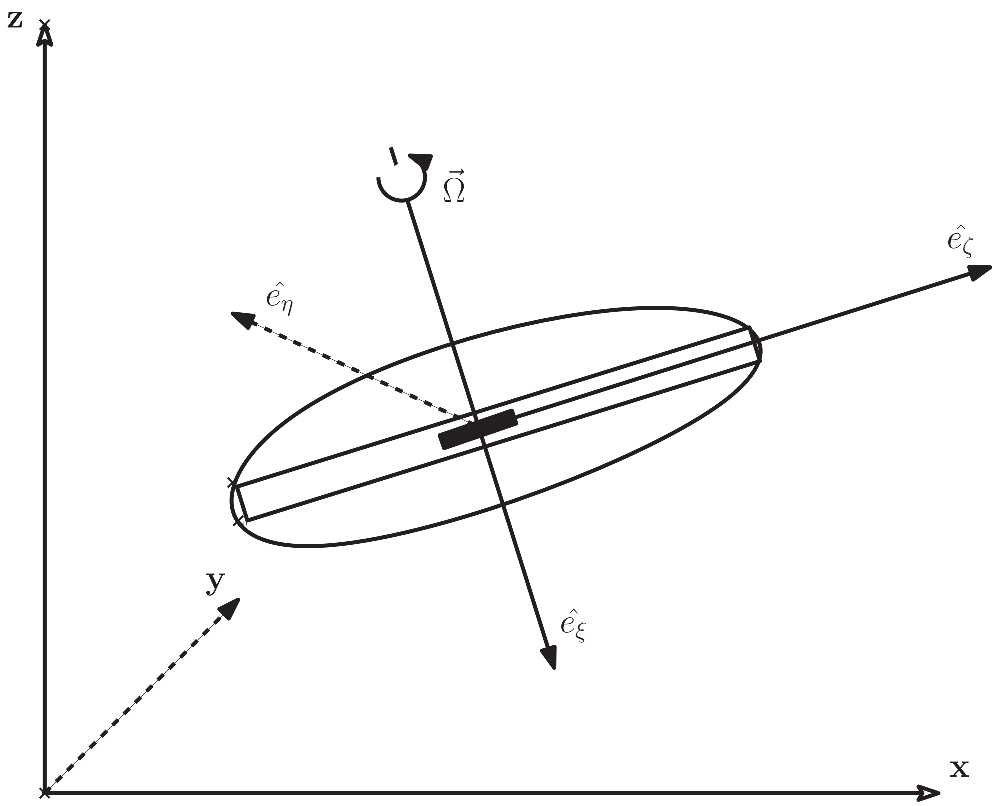


Figure 3.1 Rotor based Cartesian coordinate system

relation.

$$\begin{bmatrix} \hat{e}_r \\ \hat{e}_\theta \\ \hat{e}_z \end{bmatrix} = \begin{bmatrix} 0 & \cos\theta & \sin\theta \\ 0 & -\sin\theta & \cos\theta \\ 1 & 0 & 0 \end{bmatrix} \times \begin{bmatrix} \hat{e}_\xi \\ \hat{e}_\eta \\ \hat{e}_\zeta \end{bmatrix} = \mathbf{M_2} \times \begin{bmatrix} \hat{e}_\xi \\ \hat{e}_\eta \\ \hat{e}_\zeta \end{bmatrix} \tag{3.5}$$

In case the rotor blade has a deflection with respect to the plane of rotation [1], we further define a blade fixed coordinate system $(n, \theta, s)$, where $s$ is in the spanwise direction of the blade or in other words, it is the locus of the centers of pressure of the airfoil sections. $\hat{e}_\theta$ is the same as in the previous system and $\hat{e}_n$ is defined to complete the right handed system. A curved blade is depicted in Fig. 3.3.

Thus, the $(n, s)$ axes always lie in the $r$-$z$ plane and if there is no deflection i.e. $\delta = 0$, then the $n$ axis becomes opposite to $z$ while the $s$ axis coincides with $r$. The transformation between

[1]Since the current procedure does not model the structural dynamics of the blades, the deflections, if any, need to be specified apriori.

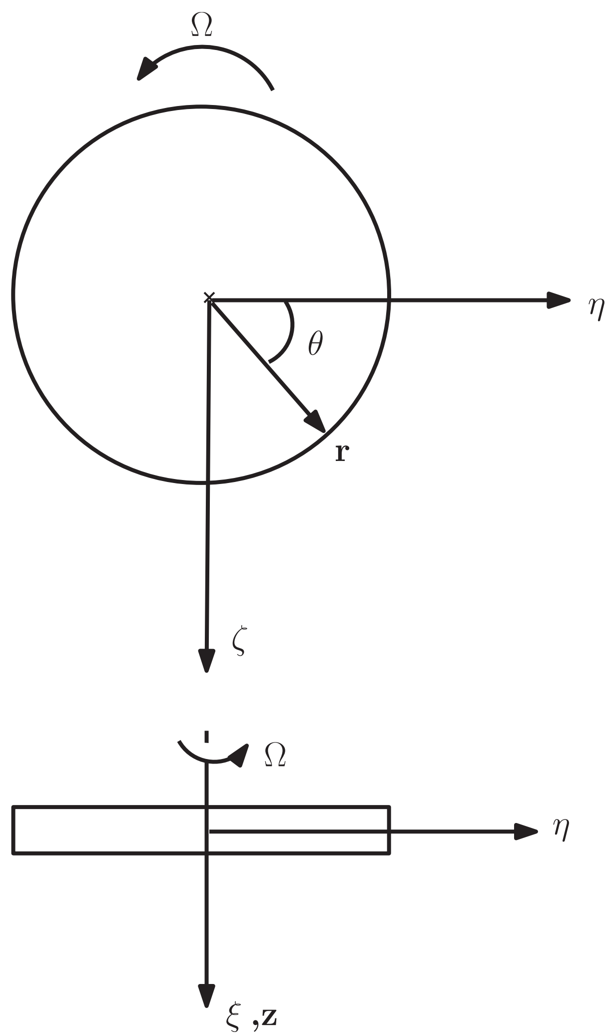


Figure 3.2 Rotor based cylindrical coordinate system

this system and the cylindrical system can be written as:

$$\begin{bmatrix} \hat{e}_n \\ \hat{e}_\theta \\ \hat{e}_s \end{bmatrix} = \begin{bmatrix} \sin\delta & 0 & -\cos\delta \\ 0 & 1 & 0 \\ \cos\delta & 0 & \sin\delta \end{bmatrix} \times \begin{bmatrix} \hat{e}_r \\ \hat{e}_\theta \\ \hat{e}_z \end{bmatrix} = \mathbf{M_3} \times \begin{bmatrix} \hat{e}_r \\ \hat{e}_\theta \\ \hat{e}_z \end{bmatrix} \tag{3.6}$$

If the distribution of deflection along the blade is given, then the following equation of a curved blade can be used:

$$\vec{\mathbf{R}}(s) = \hat{e}_r \int_0^s \cos\delta(s)\ ds + \hat{e}_z \int_0^s \sin\delta(s)\ ds \tag{3.7}$$

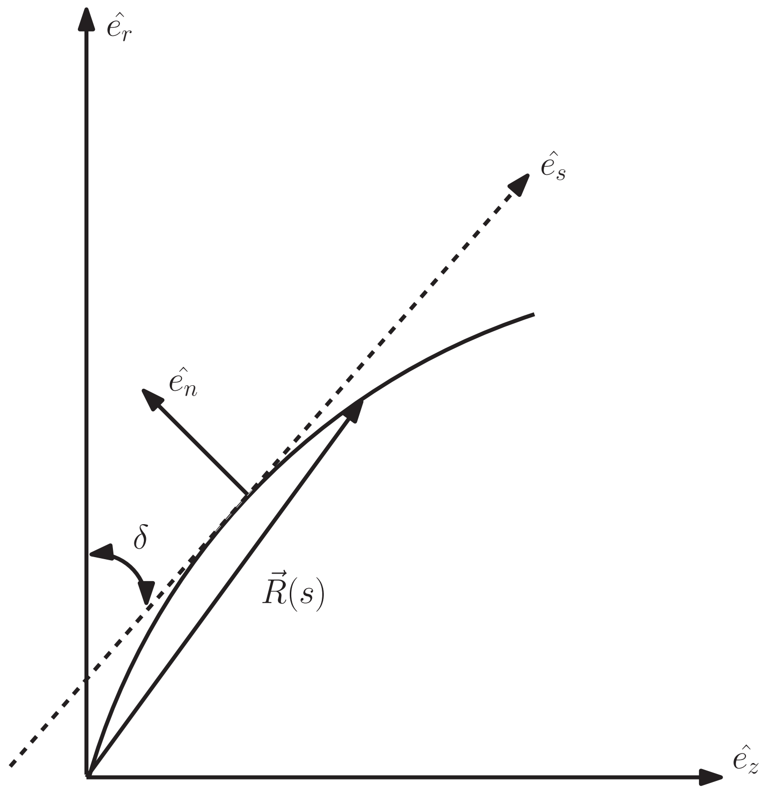


Figure 3.3 Curved blade

### 3.3.2 Rotor Discretization and Intersection

In this section, we shall discuss how the rotor is discretized and subsequently, explain the method of finding the rotor's intersection with the tetrahedral grid elements.

#### 3.3.2.1 Rotor Discretization

The unsteady rotor model considers the rotor to be made up of discrete blades and not as a simplified solid disk. The rotor blades are discretized into elements in the form of circular arcs, centered at the rotor center (See Fig. 3.4).

Blade properties such as blade chord, thickness, twist, out of plane deflection and cross sectional characteristics at the center of the element are assumed to prevail over the entire element. Each of these blade elements acts as a source of momentum, with the source assumed to be concentrated at the center of the element. Thus, each rotor blade behaves as a discrete line of momentum sources. For obtaining a time-accurate solution, it is required to trace

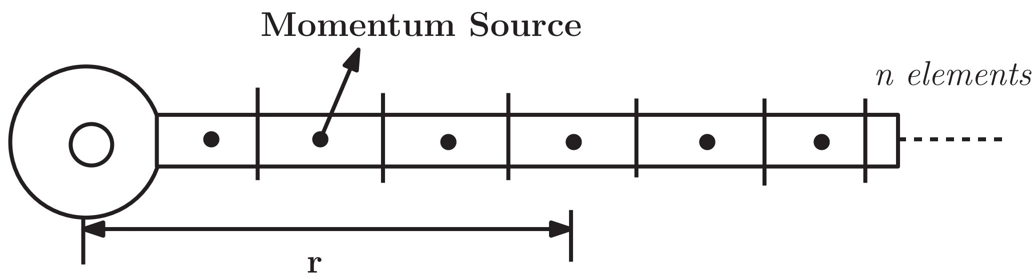


Figure 3.4 Rotor discretization

the time-dependent position of these blades and accordingly find their intersections with the computational grid. The blade position is simply taken to vary linearly with time i.e. the azimuthal position of each rotor blade is given by:

$$\psi = \Omega * time \tag{3.8}$$

#### 3.3.2.2 Rotor Intersections

It is evident that the main feature of the unsteady rotor model is that the instantaneous position of each rotor blade is determined at every instant in time and the rotor intersections are accordingly found. Each of the blade elements travel in an arc about the rotor center. Such an arc described by each blade element is oriented arbitrarily with respect to the three-dimensional computational domain, thereby making the process of finding intersections between the rotor and the computational domain difficult.

In the current research, the computational domain is made up of tetrahedral grid elements. We, therefore, have to find the intersection of an arc with tetrahedrons. The algorithm for finding the rotor intersections defines a natural coordinate system for each tetrahedron. Given a blade location i.e. the $(r, \theta, z)$ coordinates of a blade section, we find which tetrahedron that section lies in by transforming its polar coordinates to the tetrahedral based natural coordinates [**?** ]. We begin by finding the starting cell at a given time step and continue till all the tetrahedrons intersected by a particular blade, in that time step, are found. The angle subtended by a blade section at the rotor center while traversing through a tetrahedral element is computed and stored. This process is repeated for every discretized section of a blade, thereby giving all the possible intersections of the rotor with the computational domain at a given instant in time.

At this point, the difference between the steady and the unsteady rotor model is worth emphasizing again. The main distinction between the steady rotor model and the discrete blade unsteady rotor model is that in the latter, the rotor source terms are added only to those specific control volumes where the rotor blades are actually present, leaving out the rest of the rotor disk plane. For example, for a 2-bladed rotor, if one blade is located at an azimuthal position of $\psi$ at a given instant in time, the other blade would be at $\psi + 180^0$. Then the rotor source would be added to only the control volumes around these two specific regions.

#### 3.3.2.3 Time Step Requirement

After determining the tetrahedral elements where the rotor source has to be added, the question now arises as to how much of the rotor source term should be added to each of these specific cells. It might so happen that at the start of a time step, a blade is present at a position halfway through a tetrahedral element and by the end of that time step, it traverses that element plus half of the next element. A more general scenario would be where a blade line traverses through $x$ number of elements within one time step, some completely while others only partially. It would be erroneous to add the full magnitude of the rotor force to the elements which have only been traversed partially. We, therefore, find the $\Delta\theta$ distance that a blade line travels while passing through a tetrahedral element and average it by the total angular distance $(\Omega * \Delta t)$ that the blade travels in a particular time step. The unsteady source term to be added to a tetrahedral element takes the form:

$$\vec{S} = \frac{\Delta\theta}{\Omega\Delta t}\{-\vec{F}\} \tag{3.9}$$

where, $\Delta\theta$ is the angular distance that the blade traverses in passing through a tetrahedral element. If we take a very large value of the time step such that $\Omega\Delta t = 2\pi$, which means that a blade completes one revolution in one time step, it can be seen that Eq. 3.9 becomes the same as Eq. 3.1, which is used for a steady rotor with one blade ($N_b = 1$). The unsteady rotor model then collapses into the steady rotor model, for now the rotor source terms are added throughout the disk plane. The steady rotor model can, therefore, be viewed as a limiting case of the unsteady rotor model.

It is evident that the choice of the time step is crucial in this method. A good choice of the time step would be one where a blade takes more than one time step to travel through one grid cell. In other words, the time step should be adequately small so as to ensure that a blade does not jump through more than one grid cell in a time step. The idea here is to make the ratio ($\Delta\theta/\Omega\Delta t$) tend to one so that there is no averaging involved (See Figs. 3.5 and 3.6). These requirements are met by choosing the time step such that the blade tip travels by a distance equal to $n^{th}$ fraction of the chord length at the tip. For the present computations, $n = 0.5$. Thus,

$$\Delta t = \frac{0.5 c_{tip}}{\Omega R} \tag{3.10}$$

Even for a tapered blade, since the chord length at the tip is the minimum, we can see that Eq. 3.10 furnishes a minimum usable $\Delta t$.

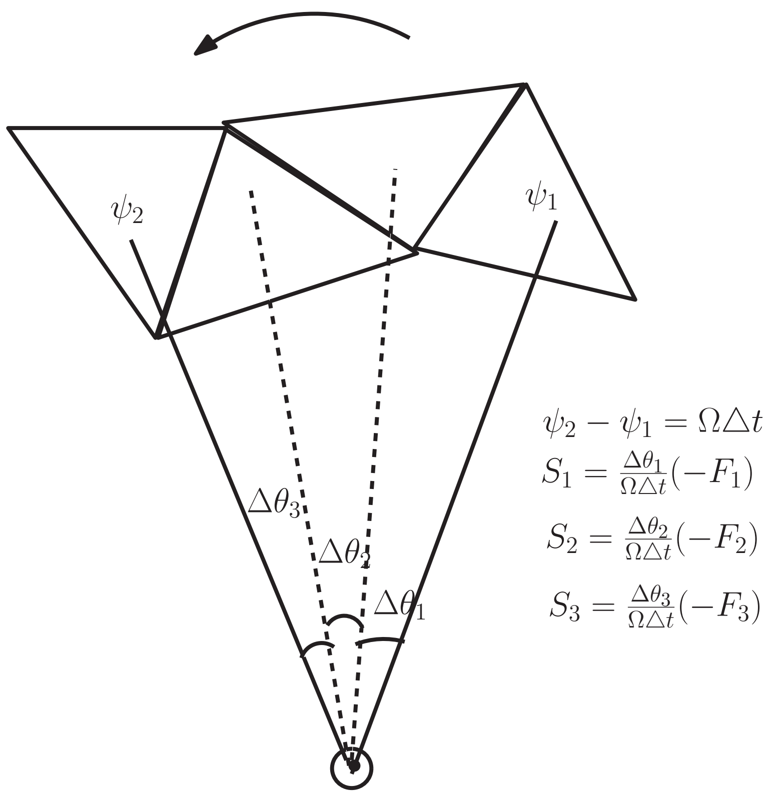


Figure 3.5 Blade traversing through multiple grid cells in one time step

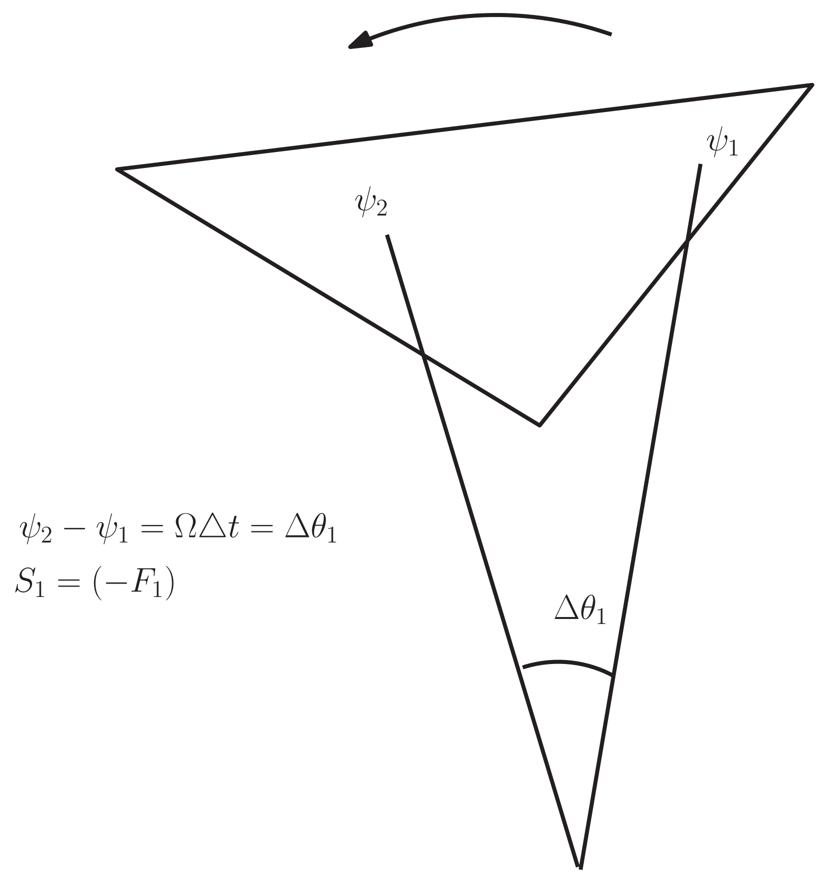


Figure 3.6 Blade remains in one grid cell for more than one time step

## 3.4 Calculation of Rotor Forces

The task now is to find the magnitude of the rotor force $\vec{F}$. Let the fluid velocity at any point '$s$' on a blade at an angular position $\theta$ be:

$$\vec{V} = u\hat{\imath} + v\hat{\jmath} + w\hat{k} \tag{3.11}$$

Using Eqs. 3.3, 3.5 and 3.6, the same velocity can be written in the $(n, \theta, s)$ system as:

$$\vec{V} = v_s\hat{e}_s + v_\theta\hat{e}_\theta + v_n\hat{e}_n \tag{3.12}$$

where,

$$\begin{bmatrix} v_n \\ v_\theta \\ v_s \end{bmatrix} = \mathbf{M_3M_2M_1} \begin{bmatrix} u \\ v \\ w \end{bmatrix}. \tag{3.13}$$

The blade also has a velocity due to its rotation which can be written in the $(n, \theta, s)$ system as:

$$\vec{V}_{bl} = \mathbf{M_3 M_2 M_1} \left( \vec{\Omega} \times \bar{\mathbf{R}}(s) \right) \tag{3.14}$$

where, $\vec{\Omega}$ is as defined in Eq. 3.2 and $\vec{\mathbf{R}}(s)$ is the position vector of the point on the blade under consideration. Thus, the relative velocity $\vec{V}_{rel} = v'_s \hat{e}_s + v'_\theta \hat{e}_\theta + v'_n \hat{e}_n$, seen by the blade is:

$$\begin{aligned} \vec{V}_{rel} &= \vec{V} - \vec{V}_{bl} \\ &= \mathbf{M_3 M_2 M_1} \vec{V} \\ &- \mathbf{M_3 M_2 M_1} \left( \vec{\Omega} \times \vec{\mathbf{R}}(s) \right) \end{aligned} \tag{3.15}$$

The aerodynamic force acting in the spanwise direction is zero and therefore, only the velocity component in the plane normal to $\hat{e}_s$ is required for evaluating the aerodynamic forces. The angle made by this component with the $\hat{e}_\theta$ direction is given by (see Fig. 3.7)

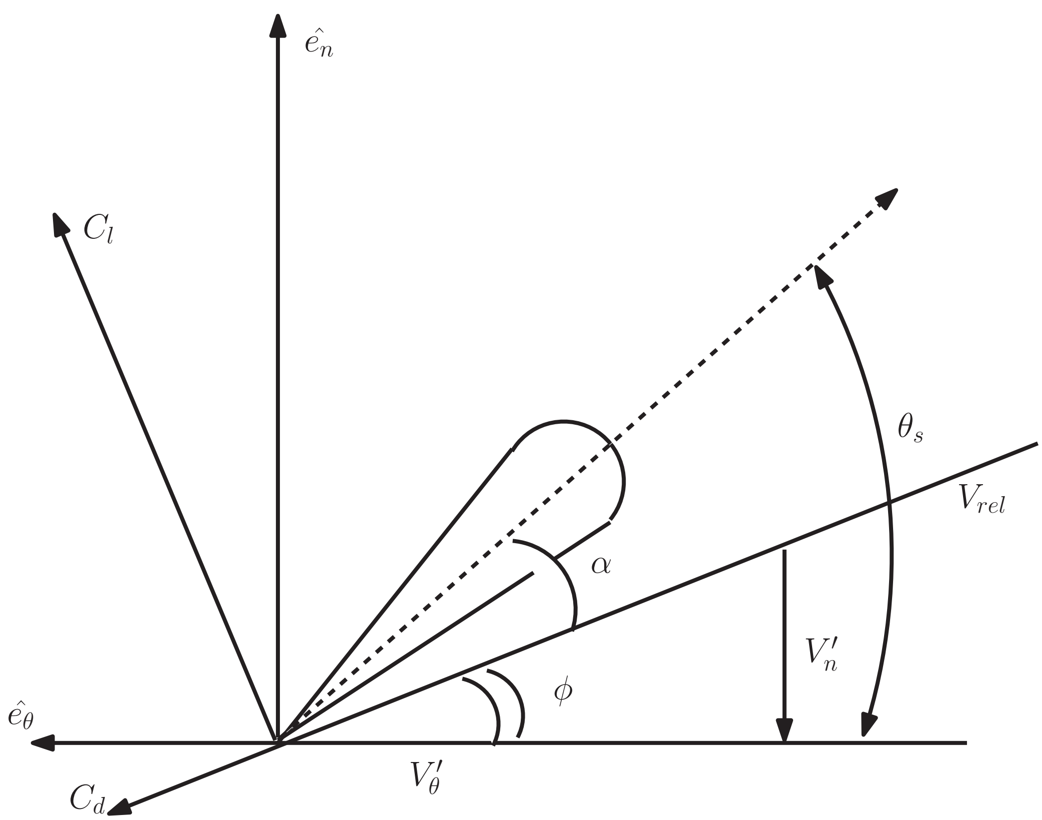


Figure 3.7 Airfoil cross-section

$$\phi = \arctan(-v'_n/v'_\theta) \tag{3.16}$$

If the section has a twist of angle $\theta_s$ with respect to the plane of rotation then, from Fig. 3.7, the effective angle of attack seen by the airfoil is:

$$\alpha = \theta_s - \phi \tag{3.17}$$

Once the effective angle of attack $\alpha$ and the components of the relative velocity seen by the airfoil are known, we can find the sectional aerodynamic coefficients $C_l$ and $C_d$ using the airfoil characteristics. The lift and drag forces can now be found from the aerodynamic coefficients.

$$\mathrm{L}' = \frac{1}{2}\rho v'^2 C_l c \; ds \tag{3.18}$$

$$\mathrm{D}' = \frac{1}{2}\rho v'^2 C_d c \; ds \tag{3.19}$$

where, c is the blade chord-length and $v'^2 = {v'_n}^2 + {v'_\theta}^2$. The lift and drag forces act perpendicular and parallel, respectively, to the relative velocity vector. Resolving these forces gives the forces in $\hat{e}_n$ and $\hat{e}_\theta$ directions.

$$f_n = \mathrm{L}' \cos\phi - \mathrm{D}' \sin\phi \tag{3.20}$$

$$f_\theta = \mathrm{L}' \sin\phi + \mathrm{D}' \cos\phi \tag{3.21}$$

Also, $f_s = 0$.

The aerodynamic forces $(f_n, f_\theta, f_s) = \vec{f}$ on the blade element can now be transformed back to the computational coordinate system $(x, y, z)$ using the inverse transformation relations.

$$\vec{F} = \mathbf{M_1}^{\mathrm{T}} \mathbf{M_2}^{\mathrm{T}} \mathbf{M_3}^{\mathrm{T}} \vec{f}. \tag{3.22}$$

$\vec{F}$ is the resultant force acting on a blade element at $(s, \theta)$, then $-\vec{F}$ is the instantaneous force acting on the fluid element at that location. The rotor force thus obtained is used in Eq. 3.9 to determine the instantaneous momentum source due to the rotor.

## 3.5 Rotor Source Terms in the Momentum Equations

The rotor sources found in the previous section are added to the tetrahedral elements that are intersected by the rotor blades. Since the discretized momentum equations are written in terms of the node points, and not the tetrahedral elements, we need to decide how this rotor source contribution will be accounted for the nodes of an intersected tetrahedron. The source term gets divided equally between the four nodes of a tetrahedron i.e. one-fourth of the momentum source, which is constant over a tetrahedral element, gets added to the discretized momentum equations of the four nodes which make up that tetrahedron. It must be noted here that a tetrahedron can be intersected by more than one blade section, in which case there will be more than one rotor source contribution to the discretized momentum equations for the node points of the concerned tetrahedron. It is good practice to discretize a rotor blade such that there are about 100 momentum sources along a blade radius.

In the next chapter, the validation results for the unstructured median-dual based flow solver are discussed. This will be followed by the validation results for the unsteady rotor model, obtained by testing the unsteady rotor model with an already available 3D structured code. It must be noted here that since both the structured and unstructured flow solvers use finite volume based SIMPLER algorithm, the coupling process of both the rotor models is quite similar. The difference is in the procedure of finding the rotor intersections as the type of grid cells varies between the structured (Cartesian hexahedral elements) and the unstructured (tetrahedral elements) flow solvers. The following flowchart summarizes the discrete blade unsteady rotor model and its coupling with an unsteady flow solver, be it structured or unstructured.